Full-Field Measurement of Strain and Transformation in Nitinol

K. E. Perry[1], P. E. Labossiere[1] and E.S. Steffler[2]
[1]ECHOBIO LLC, Bainbridge Island, WA, USA
[2]Idaho National Engineering Laboratory, Idaho Falls, ID USA

Abstract

Phase shifted moiré interferometry is used to measure full-field strain during uniaxial tension and four point bend loading of nitinol test samples. Differences between global and full field measurements reveal the effects of localized transformation behavior. Results for two heat treatments of commercially available superelastic Nitinol are presented for tests conducted under controlled temperature conditions. The results highlight the effect of martensite, austenite and R-phase transformations on the thermomechanical response of superelastic nitinol. Finally, the technique is applied to a nitinol implantable medical component to demonstrate the opportunities for improved material characterization, numerical modeling and design validation.

Introduction

The deformation behavior of nitinol is complicated by a number of factors attributed to the materials unique multi-phase composition. Tension/compression asymmetry, phase boundary localization loading and temperature history all contribute to the complexity of the deformation response of nitinol. In this work, we present detailed measurements of deformation and strain for two material heat treatments and several modes of loading. Using a novel sample geometry, both uniaxial tension and four point bending deformation modes are studied at a range of temperatures both above and below the A_f temperature.

The photomechanics method that we have adopted and fine-tuned provides both real-time and high resolution full-field deformation analysis and is exceptionally suited for characterizing nitinol coupon samples. We demonstrate the ability to simultaneously determine strains in the various material phases at a rate of 15 non-interlaced frames per second and a resolution of 1280x960 and 10 bit depth resolution. The custom loading and measurement system is capable of capturing the behavior over a wide temperature range allowing for studies of both superelastic and shape memory properties.

Materials and Experiment

The material used in this study was SE-508, seamless drawn tubing from Nitinol Devices and Components, Inc. with an as-received A_f of -9°C. Two distinct additional heat treatments were chosen, denoted by A and B. Treatment A was performed at 325°C for 60 minutes and treatment B was performed at 500°C for 30 minutes. All samples were water quenched subsequent to heat treating and A_f tested following the ASTM F-2082 method for bend free recovery [1] as well as using DSC measurements performed by Special Metals, Inc. Samples with treatment A demonstrated a large R-phase component with two transformation peaks compared to the single transformation peak visible upon cooling for samples with treatment B.

A single sample geometry was chosen that allowed for both uniaxial tension and four-point bending test configurations. Figure 1 is a schematic of the sample geometry showing the four laser cut holes used to pin load the sample, the EDM cut windows to reveal the “gage” section and the flattened face which was carefully ground and polished to receive the 300 l/mm diffraction grating for moiré interferometry. Prior to production of the samples, FEA was used to optimize the design of the sample geometry and the corresponding fixtures to achieve

uniform tension and pure bending over a large range of deformations. A slow loading rate (<1 mm/min) was used for all of the tests.

Global (Far-field) measurements of the sample load, extension and displacement were made using a load cell, extensometer with a gage length of 10mm and LVDT, respectively. A minimum of two thermocouples were used to monitor the sample temperature throughout the experiments and temperature control was provided by directing a laminar flow of chilled or warmed air within the range from -30 to 40 ^{o}C over the sample. The samples were loaded in either tension or bending using a custom built load frame and fixturing. Figure 2 shows a photograph of the load frame mounted on an optical table with the moiré interferometer and imaging system. Only two of the four beams are shown here for clarity. The experiments employed two personal computers, one each for the data acquisition and imaging systems. Load, deflection and extension measurements were digitized to 16 bits and recorded using a conventional data acquisition system at 50 Hz. Calibration for all sensors was performed to insure accurate measurements.

Phase shifted moiré interferometry was used to capture displacement fields in the form of fringe patterns during the course of the experiments [2,3]. Real time displacement and strain measurements were made at 15 (non-interlaced) frames per second with 1280x960 and 10 bit depth resolution.

Figure 1: Schematic of the sample geometry.

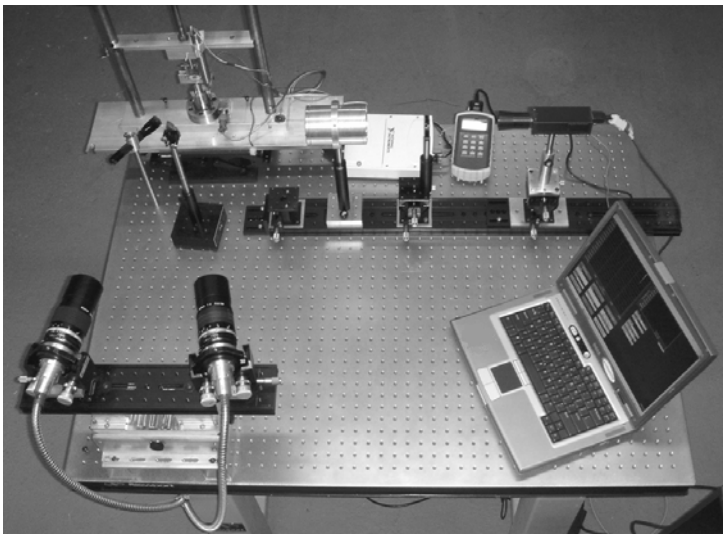

Figure 2: Photograph of the load frame and two beams of the phase shifting moiré interferometer.

Superelastic Uniaxial Loading and Unloading

Uniaxial tension tests were fist conducted at temperatures above the A_f for both heat treatments. Samples were loaded until the formation of localized deformation zones, usually initiating at one or both of the ends of the sample gage length. Figure 3 is a series of representative fringe patterns showing the loading of a typical sample when tested above A_f. Figures 3a-c correspond to loading levels below the transformation stress while Figure 3d shows localization occurring at both ends of the sample. Uniaxial loading of samples of both Treatment A and B exhibited localization when tested above A_f and demonstrated full recovery upon unloading. Figure 4 is a representative fringe pattern for treatment B during unloading where carrier fringes have been added to resolve the strain field in both the parent and transformed phase of the material. The parent phase, on the left in the figure presents smooth fringe contours while the transformed material on the right hand side exhibits coarser fringes. Figure 5 plots the applied stress versus local strain measurements for treatment B along with the corresponding extensometer strain recorded during the test.

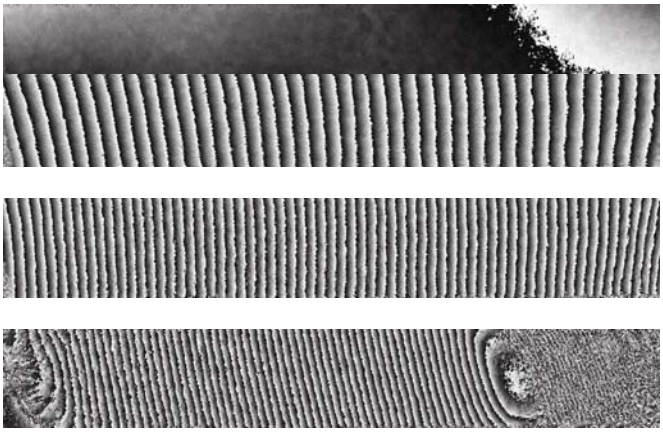

Figure 3: Representative series of wrapped fringe patterns for uniaxial tensile loading at a temperature above A_f.

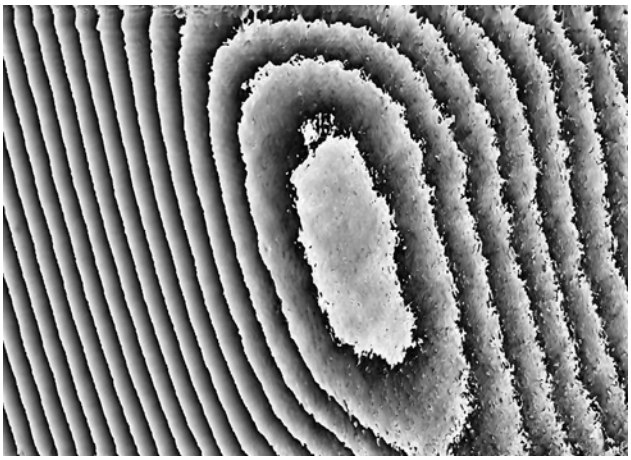

Figure 4: Fringe pattern captured during unloading where carrier fringes have been used to simultaneously resolve the strain in both material phases.

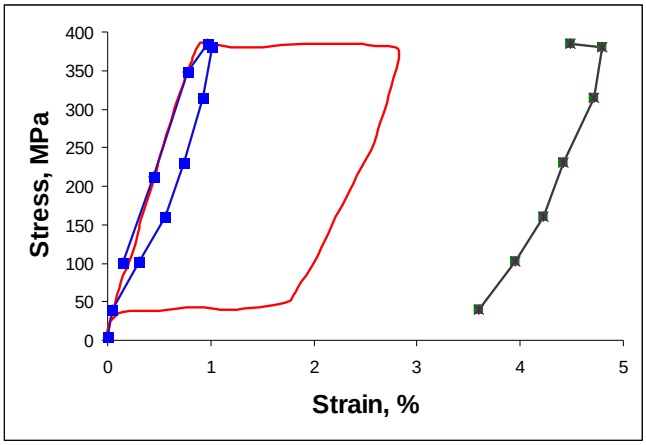

Figure 5: Applied stress versus local strain measurement with the corresponding extensometer strain recorded during testing.

Two-way Shape Memory Measurement and Coefficient of Thermal Expansion

After a single loading and unloading cycle above A_f, a small two-way shape memory strain was observed for the sample having treatment B. At the top of Figure 6 is a fringe pattern illustrating the temperature induced deformation at the right hand side of the sample of 0.37% strain when this sample underwent a change in temperature from 26°C to -18°C. The location of this strain corresponds to the end of the sample that previously experienced localization when loaded and unloaded above A_f. For the remainder of the sample, the strain was slightly negative with a value corresponding very close to that anticipated for the coefficient of thermal expansion for martensite. Figure 6 also shows a strain contour plot (middle) and strain value histogram (bottom). The strain value histogram plots the number of material points having each strain value for the range of values used in the strain contour plot (middle). While we do not present here a systematic study of the training and measurement of two-way shape memory components, these results serve to demonstrate the capabilities and accuracy of our measurement technique.

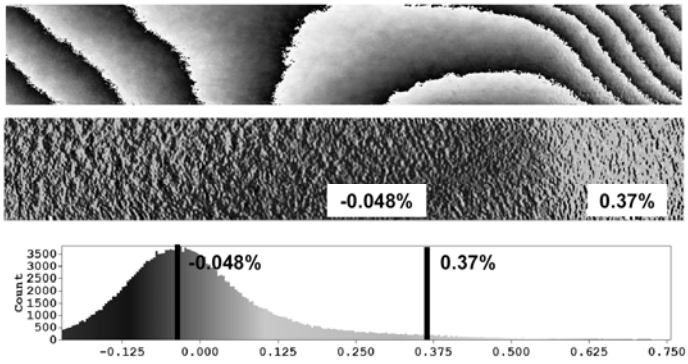

Figure 6: Fringe pattern (top), strain contour plot (middle) and strain value histogram (bottom) for a two-way shape measurement.

Uniaxial Loading and Thermal Recovery

After cooling to below -18°C, samples of both heat treatments were loaded and unloaded in uniaxial tension. In the case of the sample with treatment A, localization occurred at one end of the sample. No significant localization was observed for samples with treatment B, although localization did occur in

these samples at temperatures above A_f. After the samples were unloaded, they were allowed to warm to room temperature under a controlled rate of approximately 2 degrees per minute. Figure 7 shows a series of fringe patterns for the typical free recovery of a uniaxial test sample for Treatment A. Between -18°C and -2°C the localized region decreased slightly in size while the remainder of the sample experienced a gradual decrease in strain. Between -2°C and 0.6°C the localized region quickly disappeared while the gradual strain decrease continued until the sample was retuned to above its A_f temperature.

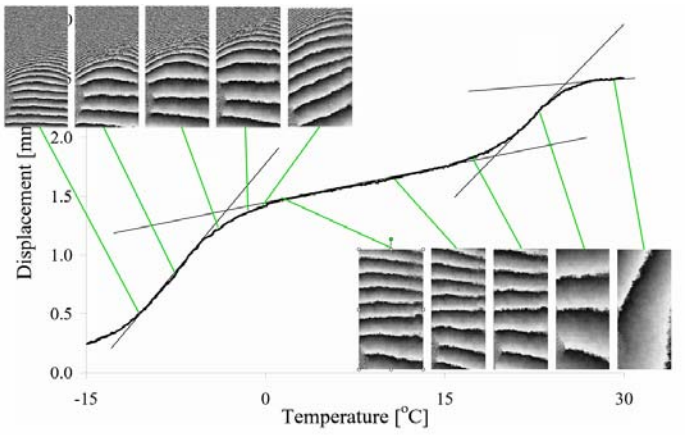

Figure 6: Series of fringe patterns showing the thermal recovery and the active A_f curve for samples with treatment A.

Four Point Bend Loading

Figure 8 shows typical fringe patterns for a sample in four point bending above the critical stress for transformation. In all cases, the fringes clearly indicate an asymmetric neutral axis, even at stress levels below the critical transformation stress. Furthermore, detailed analysis confirmed that the axial strain distribution was linear from the top edge to the bottom edge of the samples, therefore it is concluded that the asymmetry between tension and compression for these samples results from an asymmetry in the modulus of the parent phase. Figure 8 shows a localization band that has formed in the upper right hand corner of the image.

Figure 9 shows a plot of load versus strain measurements for a location at the top edge of the sample and at a location along the bottom edge for a completely reversed cycle of forward/reverse bending. The slope differences in tension versus compression can be seen as well as the full recoverability of the material at these test temperatures.

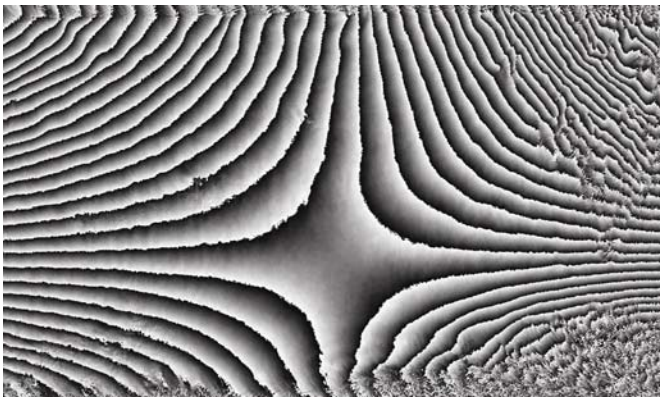

Figure 8: Fringe pattern for a sample under four-point bend loading above the stress for phase transformation.

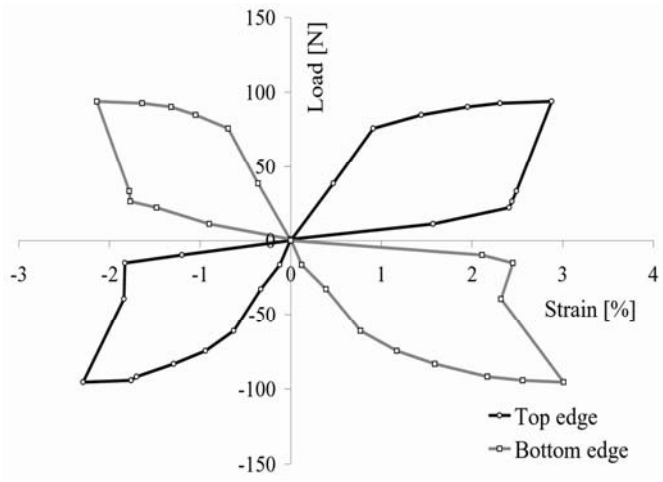

Figure 9: Applied load versus local strain measurements from the top and bottom edges of a sample loaded through a fully reversed bending cycle.

Component Scale Measurements

Component scale measurements were made on a typical nitinol stent strut pair. The width of the struts was nominally 300 microns and the sample was shape set flat and polished to receive a diffraction grating. The sample was loaded by deforming the struts and imposing a fixed spacing between them to simulate uniform radial compression loading of 10% and 20% from the

original expanded diameter. Figure 10 shows three fringe patterns corresponding to no load, 10% and 20% radial compression. At peak loading, maximum tensile strains are associated with the outer edge of the sample while peak compressive strains are located along the inner edge of the apex radius. Discontinuities in the fringe patterns were observed on both the tensile and compressive edges of the sample.

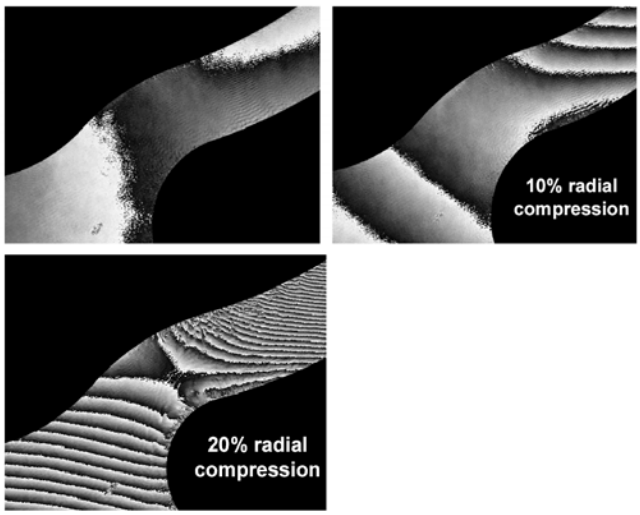

Figure 10: Series of fringe patterns for a typical nitinol strut pair under simulated radial compressive loading.

Discussion

A real time, full field technique for directly measuring displacements and strains has been demonstrated for uniaxial tensile and four point bend loading of a nitinol coupon sample. The novel sample geometry permits detailed studies of the differences between material with different processing histories over a wide range of temperature and loading conditions. Uniaxial tensile tests at temperatures above A_f clearly reveal the multiphase nature of the material with discrete strain values associated with each phase. Different behaviors were observed for the two material heat treatments when the samples were deformed at -18°C, with the treatment A samples showing a more complicated two-step reverse transformation process. Quantification of two-way shape memory strain and measurement of determination of coefficient of thermal expansion were demonstrated. Finally, the technique was applied to a typical nitinol component geometry where tension/compression asymmetry as well as phase boundary localization was observed.

References

[1] Perry et. al., Thermoelastic Transformation Behavior of Nitinol, *American Society for Testing and Materials JAI 9040/STP 1481*, accepted for publication

[2] D. Post et. al., *High Sensitivity Moiré*, Springer-Verlag, 1994

Acknowledgements

The authors would like to gratefully acknowledge the contributions of Randy Lloyd and Nate Stevens of the Idaho National Engineering Laboratory, Frank Scerzenie of Special Metals, NDC and Matt Will of EDM Tek.